

LP Compressor Blade Vibration Characteristics at Starting Conditions of a 100 MW Heavy-duty Gas Turbine

An Sung Lee*

*Rotor Dynamics Group, Korea Institute of Machinery and Materials,
Daejeon 305-600, Korea*

Alexandre F. Vedichtchev

*Gas Turbine Department, Leningradsky Metallichesky Zavod
Baskov 26, 191914, St. Petersburg, Russia*

In this paper are presented the blade vibration characteristics at the starting conditions of the low pressure multistage axial compressor of heavy-duty 100 MW gas turbine. Vibration data have been collected through strain gauges during aerodynamic tests of the model compressor. The influences of operating modes at the starting conditions are investigated upon the compressor blade vibrations. The exciting mechanisms and features of blade vibrations are investigated at the surge, rotating stall, and buffeting flutter. The influences of operating modes upon blade dynamic stresses are investigated for the first and second stages. It is shown that a high dynamic stress peak of 120 MPa can occur in the first stage blades due to resonances with stall cell excitations or with inlet strut wake excitations at the stalled conditions.

Key Words: Compressor Blade Vibrations, Starting Conditions, Heavy-Duty Gas Turbine, Blade Dynamic Stresses, Surge, Rotating Stall, Buffeting Flutter, Stalled Oscillations

Nomenclature

C_z : Mean axial flow speed
 H : Stage work
 u : Blade tip speed
 n : Compressor rotating speed
 \bar{n} : Relative compressor speed, n/n_{des}
 \dot{m} : Mass flow rate
 \dot{m}_{eq} : Equivalent mass flow, $\dot{m}\sqrt{T_i}/P_i$
 P : Total pressure
 P_r : Pressure ratio, P/P_i
 T : Temperature
 Ψ : Pressure coefficient, $2H/u^2$
 φ : Flow coefficient, C_z/u
 $\bar{\varphi}$: Relative flow coefficient, φ/φ_{des}

Subscripts

des : At the design point
 eq : Equivalent
 i : Inlet

1. Introduction

It is well known that the starting conditions are very dangerous for lower stage blades in multistage axial compressors of gas turbines. The problems had appeared firstly in the mid 40s, when many blade failures had occurred at the first two lower stage blades in axial compressors of aircraft gas turbines (Shannon, 1954). To investigate the blade failures many complex vibration and aerodynamic investigations had been carried out, using the stationary static cascade models, and the rotating model and full-scale compressors. They had identified the rotating stall and stalled flutter, which had been unknown at that time, as the main sources of the problems. These

* Corresponding Author,

E-mail : aslee@kimm.re.kr

TEL : +82-42-868-7356; FAX : +82-42-868-7440

Rotor Dynamics Group, Korea Institute of Machinery and Materials, Daejeon 305-600, Korea. (Manuscript

Received March 11, 2003; Revised February 13, 2004)

non-stationary phenomena usually occur at lower stage compressor blades at the part load or starting conditions, and they induce high dynamic stresses in fundamental flexural modes, which may result in immediate high cycle fatigue failures. Rusanova (1958) was one of the firsts who had measured the dynamic stresses of blades at the starting conditions in the multistage axial compressor. Detailed experimental works of the phenomena had been introduced by Samoylovict (1975). The rotating stall vibration had been investigated explicitly by Ishihara and Funakawa (1980) and Kulagina (1976).

In subsequent investigations significant attentions had been given to identify the operating conditions at which the phenomena occur and to develop their elimination measures. As a result special measures had been applied to axial compressors and events of high cycle fatigue failures had decreased considerably (Vedichtchev and Titenskiy, 1983). However, in spite of a big advance in the technology the problems of compressor blade vibrations at the starting conditions are not completely solved, yet. Therefore, upon developing new compressors time-consuming and expensive complex vibration and aerodynamic tests need to be carried out. Besides, Ki and Chung (2002) reported the transient performance characteristics of a turboprop gas turbine, including compressor components, at the on and off design points.

In this paper are given the blade vibration characteristics at the starting conditions in the low pressure multistage axial compressor of a 100 MW heavy-duty gas turbine. A sectional view of the gas turbine is shown in Fig. 1 and its features are summarized in Table 1. For vibration and aerodynamic tests of the LP compressor a scaled model compressor has been constructed. Its scale factor of simulation is equal to 4.14. The model compressor has been tested on a test stand, using a steam turbine as a driver. Vibration data have been obtained through strain gages attached to the blades during aerodynamics tests. Observations of the blade vibrations are shown at the surge, rotating stall, and buffeting flutter. The influences of operating modes in the compressor

Table 1 Features of the 100 MW heavy-duty gas turbine

Item	Unit	Value
Power	MW	100
Turbine inlet temp.	°C	750
Pressure ratio		
- LP compressor		6.3
- HP compressor		4.25
Design speed		
- LP compressor	rpm	3000
- HP compressor		4100
Mass flow rate	kg/s	460
Number of stages		
- compressor		8+13
- turbine		3+5
Inlet diameter ratio in LP compressor		0.5
Inlet flow coefficient in LP compressor		0.486

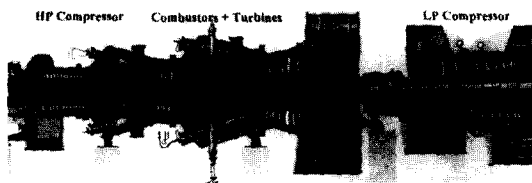


Fig. 1 A sectional view of the 100 MW heavy-duty gas turbine

stages are investigated on the intensities of stalled vibrations. The flow coefficients at the first stage, at which the stalled vibration occurs, are determined and the maximum dynamic stress intensities are obtained. The exciting mechanisms of non-stationary phenomena are also considered.

2. Operating Characteristics of Compressor at Starting Conditions

It is known that the non-stationary phenomena in axial compressors are caused by changes of flow conditions on blades at the part load or starting conditions. The operating mode of each stage in a compressor may be described by the aerodynamic performance. The performance of the first stage in the tested model LP compressor

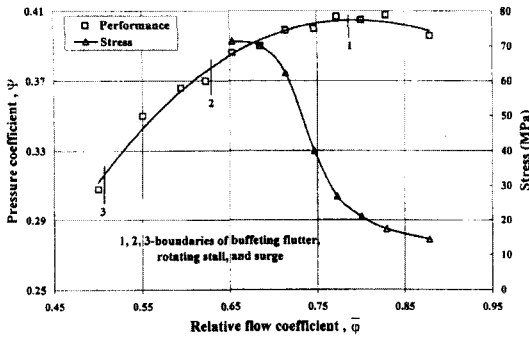


Fig. 2 Aerodynamic performance of the first stage and blade dynamic stress

is shown in Fig. 2 as the pressure coefficient, Ψ , vs. the relative flow coefficient, $\bar{\varphi}$. Where a change of the relative flow coefficient allows of estimating a change of the stage operating mode at the part load conditions.

Let's consider a change of the relative flow coefficients in various stages of the model compressor at the part load conditions. A plot of the relative flow coefficients vs. relative compressor speed, \bar{n} , is shown in Fig. 3. As the relative speed decreases further over 0.7, in the first three stages the relative flow coefficients decrease significantly and in the next three stages they change less significantly. But in the last two stages they increase noticeably. The reductions of the relative flow coefficients in the first three lower stages are much more than the increases in the last two higher stages. The observed different behaviors of the relative flow coefficients are resulted because air density does not correspond to that at the design rotating speed. The greatest decrease of air density takes place in the last stage due to the density reduction effects in the previous stages. Therefore, the increases of volume flows in the last higher stages result in the increased flow coefficients in these stages. Thus, they lead to the flow capacity limits or choking conditions in the last higher stages. As a result the flow coefficients decrease in the first lower stages. In the next middle stages the volume flow changes less significantly as the reduction of mass flow is compensated by the decrease of air density. This results in much less significant changes of the

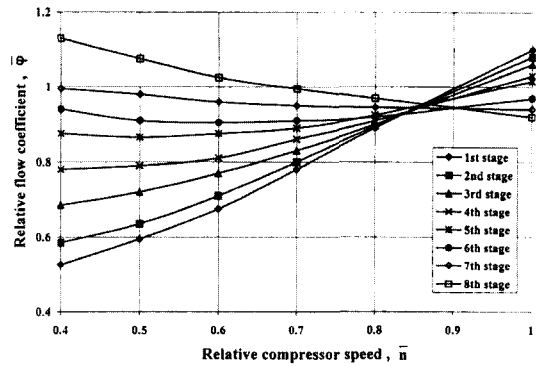


Fig. 3 Relative flow coefficients vs. relative compressor speed at various stages

flow coefficients. The larger the number of stages and the greater the pressure ratio in axial compressors, the more significant changes of the flow coefficients are resulted at the starting conditions.

A change of the flow coefficients gives rise to the incidence angle change at blades. The first stage tends to operate at the higher (positive) incidence and the last stage tends to operate at the lower (negative) incidence. In the middle stages the incidence changes in a less extent. For instance, in the first stage of the compressor the incidence can reach as high as 20° at the starting conditions as the flow coefficient decreases. Such a high incidence may cause the flow separation at blades. On the other hand, it is supposed from Fig. 3 that if the compressor speed increases above the design speed, the first stage tends to operate at the lower incidence while the last stage tends to operate more near the stall.

The stall is the main source of occurrences for the buffeting flutter, rotating stall, and surge in spite of their different exciting mechanisms (Samoylovict, 1975). All these non-stationary phenomena have been detected during aerodynamic tests of the model compressor. Their starting boundaries have been determined by measuring stream fluctuations and stress amplitudes. The boundaries are shown in Fig. 2 of the aerodynamic performance map of the first stage. It is noticed that all the non-stationary phenomena occur to the left on the performance map. As the flow coefficient decreases further from the design point value, the buffeting flutter occurs first, then

the rotating stall and finally the surge occur in turn.

3. Test Results and Discussions

Vibration and aerodynamic tests have been carried out during four different constant throttle runs with five constant compressor speeds, i.e., $\bar{n}=0.4, 0.5, 0.6, 0.7,$ and 0.8 . The lines, corresponding to these operating conditions, are plotted on the pressure ratio vs. equivalent mass flow characteristic of the compressor in Fig. 4. They divide the area of this characteristic map into many zones. Measurements have been carried out along the boundaries of these zones, and thereby almost all possible operating conditions at the part load conditions have been investigated. Vibrations have been measured through strain gauges attached to the blades surfaces near their roots. It has allowed of measuring the maximum stresses in the fundamental flexural modes of blades.

At the part load or starting conditions the main feature of blade vibrations has been the continuous existence of intensive (but no resonance) oscillations over the part speed range. Resonance oscillations occur at integer multiples of rotating speed as they coincide with blade natural frequencies. However, for these intensive oscillations all the blades in one stage simultaneously vibrate at their own fundamental natural flexural modes with their independent natural frequencies. The oscillations are very sporadic. The vibration amplitudes continuously build up to the maximums and then decrease to the minimums in the most random manner. A ratio among the maximum stresses may reach three within the blades in one stage. A typical vibration signal is shown in Fig. 5. This vibration characteristic appears almost equally for each non-stationary phenomenon. These types of blade vibrations are named simply as the stalled oscillations.

Resonance vibrations in the fundamental flexural modes at harmonics of the fixed circumferential non-uniformity or rotating stall have not caused any noticeable change to the above characteristic of stalled oscillations during tests.

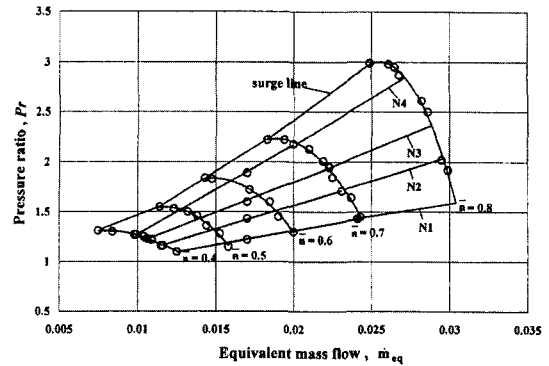


Fig. 4 Compressor characteristic and operating lines for the model compressor tests

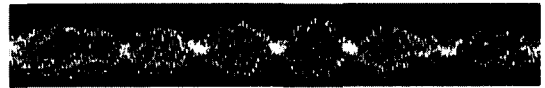


Fig. 5 A typical blade vibration signal at the stalled oscillations

Only the most intensive harmonic has increased the alternating amplitude of stalled oscillations at the resonant speed range. Thus, the majority of resonances has had no noticeable stress peaks at the resonant speeds, and they have hardly been detected on the background of permanently existing stalled oscillations.

3.1 Surge

The surge, as is known, is the most dangerous non-stationary phenomenon. At the surge the low frequency (30~60 Hz) oscillations of all air quantity in the compressor flow path may cause significant vibrations of all the units in the compressor, including bladings, casings, and branch pipes. Therefore, any compressor operating line should have a sufficient margin from the surge line for reliable compressor operation.

The surge line for the model LP compressor has been determined by observing change of the operating mode at each constant speed run. When the compressor has entered the surge condition, the test has been stopped for that constant speed run. To prevent blade breakage the compressor operating time in the surge condition has been kept as the minimum as possible. As a rule it has not exceeded ten seconds for each case. Previous

experiences of other compressor tests had shown that compressor bladings could be destroyed after operating for one minute at the surge conditions.

The surge line determined in this manner is plotted in Fig. 4 on the characteristic map. The exact determination of the surge line is very important as the compressor operating line should be kept far away enough from it. This separation or margin is represented by the stability factor which is a ratio of the compressor parameter, Pr/\dot{m}_{eq} , on the operating line to that parameter on the surge line at the same rotating speed. The minimum recommended value of the stability factor is 1.2.

Numerous tests by Samoylovict (1975) had shown that the dynamic stresses at the surge may increase up to five times of those at the normal operating modes. The stress amplification depends on the depth of entering the surge condition and compressor constructions. In the present model compressor test, taking into account the previous experiences, the deep entering of the surge condition has been avoided. Therefore, dynamic stresses in the first and second stage blades have increased only 1.5~2 times at the beginning of surge. The blades have vibrated at the fundamental flexural modes and have had unstable amplitudes. The alternating amplitudes have a stochastic characteristic and they are modulated by the surge frequency of 35 Hz. However, from a practical point of view these dynamic stresses do not cause any concern as the compressor operation is not allowed at the surge.

3.2 Rotating stall

The rotating stall has been detected in the first stage of the compressor during the constant throttle N4 run at the speed range of $\bar{n}=0.45\sim 0.7$. It has a single stall cell, rotating at 30~40 percent of the compressor speed. The rotating stall has not been detected in the second stage despite that this stage has operated in the stall conditions.

Investigations by Kulagina (1976) had shown that the stall condition is only a necessary condition but not a sufficient condition for the occur-

rence of rotating stall. The rotation of stall cell starts only at a violation of flow stability which depends on many factors. The most essential factors are the value of flow circumferential fixed non-uniformity and geometrical factors of compressor flow path, for example, inlet hub to tip diameter ratio, pitch to chord ratio, blade twist, and axial gap. Diversities of these factors and their different combinations in different stages also create the conditions for the occurrence of rotating stall in the different stages.

The excitation of oscillations at the rotating stall is due to the variable aerodynamic force on a blade that occurs as it enters and exits out the stall cell. This aerodynamic force is resulted from the incidence change on the blade from a mean value in a non-stalled area to a large positive value upon entering the stall cell and a negative value upon exiting out. This force excites oscillations of blades in both the resonant and non-resonant ways. However, the resonance excitation at harmonics of the rotating stall is most dangerous.

It is known that the resonance at the rotating stall occurs with the coincidence of blade natural frequency and stall cell excitation frequency. In such case the resonant condition is expressed as $F=(1-\bar{\omega})\cdot m\cdot n$. Where F is a blade natural frequency, $\bar{\omega}$ is a relative speed of stall cell, m is an integer multiple, and n is a compressor rotating speed. The fractional factor, $(1-\bar{\omega})$, causes the fractional ratio between the blade natural frequency and the shaft speed. This is the main difference between the stall cell excitation and the wake excitation, where the later occurs at harmonics of the shaft speed, i.e. $F=k\cdot n$.

The blade dynamic stress in the first stage at the rotating stall is shown in Fig. 6 as a function of relative rotating speed. The stalled oscillations with stresses of more than 60 MPa exist over the range of rotating stall. The vibration amplitude has been unstable. Stress increase or reduction has depended on the blade oscillation phase when the stall cell overtakes it. The maximum stress peak of 120 MPa occurs at $\bar{n}=0.5\sim 0.55$.

To explain this stress peak the Campbell diagram is plotted in Fig. 7. On the diagram are

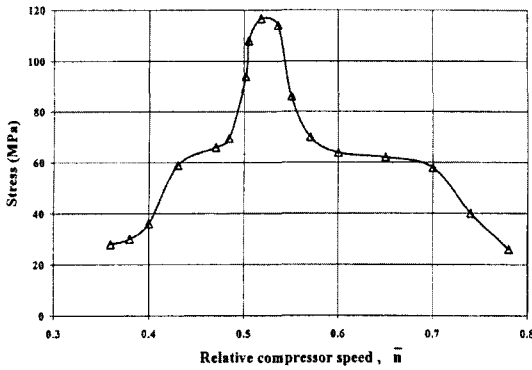


Fig. 6 Blade dynamic stress of the first stage at the rotating stall

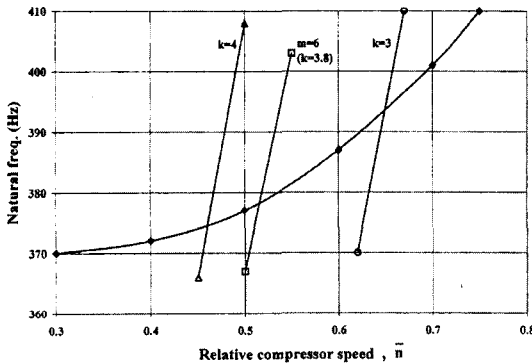


Fig. 7 Campbell diagram of the first stage blade

constructed the forcing order lines corresponding to the rotating stall cell excitation and the wake excitation of fixed circumferential non-uniformity. The line, $k=4$, corresponding to the inlet compressor strut impulses is also plotted. It can be seen that the stress peak at $\bar{n}=0.53$ is excited by the sixth harmonic of stall cell, i.e., $m=6$. In the rest of the area, where the rotating stall still exists, the resonant excitation has not taken place.

3.3 Buffeting flutter

Tests of the model compressor have shown that in a wide range of part load conditions even with the absence of rotating stall the first two lower stages blades permanently vibrate in their own fundamental flexural modes. The intensities of oscillations have been high enough. The vibration characteristics are the same as that of the

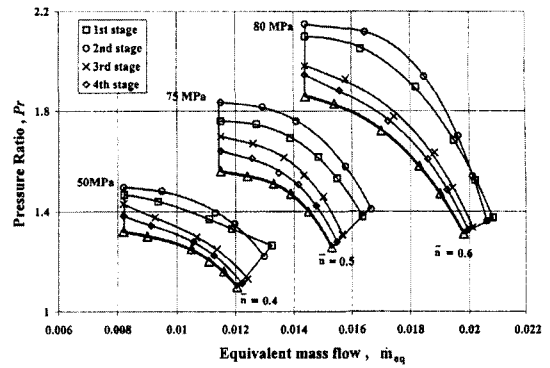


Fig. 8 Maximum blade dynamic stresses of the first to fourth stages for different throttle runs along three constant speed lines

rotating stall. These vibrations may be treated as the buffeting flutter.

The buffeting flutter vibrations have been investigated between the constant throttle N1 and N3 runs at three constant speeds. The measured maximum stresses at the first to the fourth stage blades are superimposed on the compressor pressure ratio vs. mass flow characteristic in Fig. 8. They are plotted at their corresponding operating points, ' Δ ', normal to the constant speed lines along which they have been observed. It is noticed that over all the operating ranges the dynamic stresses of the first and second stages blades are higher than those of the third and fourth stage blades.

The effects of operating modes are analyzed on the intensity of stalled oscillations. In Fig. 2 the dynamic stress of the first stage blades is plotted as a function of the relative flow coefficient along with the pressure coefficient. It is seen that the stalled oscillations occur over the transition region from the right hand side to the left hand side of the performance map. At $\bar{\varphi}=0.8$ to 0.7 the intensity of stalled oscillations increases sharply. As $\bar{\varphi}$ decreases further, there happens no significant change of stress. However, the next sharp increase of stress may arise only at the occurrence of rotating stall or surge. Detailed aerodynamic and vibration investigations on cascade blades by Samoylovict (1975) showed that such a minor change of stress is due to the decrease of fixed aerodynamic lift on a blade at

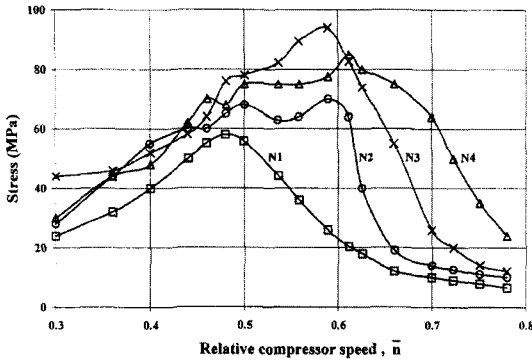


Fig. 9 Blade dynamic stresses of the second stage for different constant throttle runs

the large incidence. Thus, the performance map of the first stage in Fig. 2 has three regions corresponding to their different intensity characteristics of stalled oscillations. In the first region with $\bar{\varphi} > 0.8$ the stalled oscillations are absent, in the second region with $0.8 > \bar{\varphi} > 0.7$ they increase sharply, and in the third region with $\bar{\varphi} < 0.7$ they vary insignificantly.

The stalled dynamic stresses of the second stage blades are plotted in Fig. 9 for four different constant throttle runs as a function of the relative compressor speed. They show that the stalled oscillations exist continuously over a speed range of $\bar{n} = 0.3 \sim 0.7$. The obtained typical results are due to no significant influence of the wake resonance excitation on the stall oscillations. The starting boundary of stalled oscillations depends on each constant throttle run applied. For small throttle resistance with N1 and N2 runs the boundaries are at $\bar{n} = 0.6 \sim 0.65$, and for large throttle resistance with N3 and N4 runs they are at $\bar{n} = 0.7 \sim 0.75$. Thus, generally speaking, as the throttle resistance increases, the stalled oscillations occur at a higher relative speed and their stress intensities increase, too.

However, test results of the first stage blades in Fig. 10 suggest that such stress behavior characteristics can be changed under the influence of intensive resonance harmonic of the fixed circumferential flow non-uniformity. In Fig. 10 the dynamic stresses of the first stage blades are plotted for three different constant throttle runs as a function of the relative compressor speed.

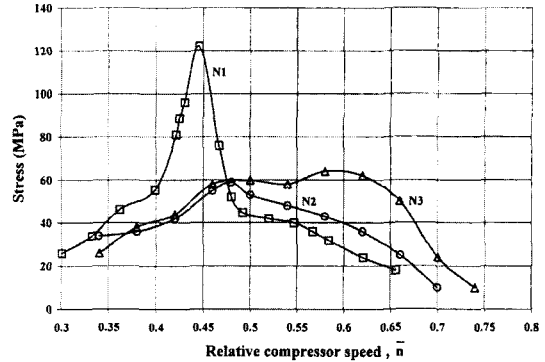


Fig. 10 Blade dynamic stresses of the first stage for different constant throttle runs Item

The maximum stress peak occurs at the minimum throttle resistance N1 run instead of higher throttle resistance N3 run as in the case of the second stage blades. The peak stress of 120 MPa occurs at $\bar{n} = 0.45$. Such a sudden stress increase has not been observed at the other constant throttle runs. The Campbell diagram in Fig. 7 shows that the peak stress is due to the resonance with the fourth harmonic equal to the number of compressor inlet struts. Thus, the resonance with the inlet strut harmonic at the stalled conditions can be dangerous for compressor rotor blades. The high stress is due to the absence of aerodynamic damping at this condition.

3.4 Exciting mechanisms of stalled oscillations

Now, consider the exciting mechanisms of stalled oscillations at the absence of rotating stall. Shannon (1954) showed that two exciting mechanisms are possible. One is a self-excited vibration such as the stalled flutter. The other is the flow separation on the suction surfaces due to the streamlining at blades with large positive incidences. The later generates variable aerodynamic forces with a broad spectrum of frequencies, and then, blades, like a filter, extract energy at frequencies equal to their own natural frequencies.

The measured stalled oscillations in the model compressor have some features of the stalled flutter. They are not resonance excited oscillations but continuous vibrations of all the blades in

the stage at their own fundamental frequencies over a broad speed range with a high level of stresses. Besides, they occur along with a transition of the stage operating mode from the right hand side to the left hand side of the performance, $\Psi(\bar{\varphi})$. Here, the transition is a possible source of the stalled flutter because airflow loses its damping properties and thereby becomes a source of self-excited oscillations. However, there are some basic differences between the measured stalled oscillations and stalled flutter. The stalled flutter has a more clearly expressed starting boundary of stalled oscillations with fast increasing amplitudes. In contrast the measured stalled oscillations have no such clearly expressed starting boundary and their amplitudes increase slowly enough. Further, the amplitudes of measured stalled oscillations have a stochastic characteristic whereas the stalled flutter has a rather steadier amplitude characteristic.

It is known that the stalled flutter occurs at a certain combination of incidence angle, flow velocity, blade material density, and blade stiffness parameter, which is a ratio of blade length to its maximum thickness (L/C). A long-term experience by Samoylovic (1975) showed that in stationary compressors with steel blades and inlet flow velocities less than 150 m/s the blade stiffness parameter should be more than 30 for the occurrence of stalled flutter. However, in the model compressor the blade stiffness parameter is much less than the critical and it is equal to 19.4 in the first stage. Such a sufficient margin of the blade stiffness parameter prevents the stalled flutter from developing in the compressor.

Thus, the following exciting mechanism of blade stalled oscillations is suggested in the absence of rotating stall. These types of oscillations are excited mainly by aerodynamic force, which results from the flow separation on the suction surface of blade at a large positive incidence. The phase difference between this force and blade movement causes an irregular amplitude change of blade vibration. On the other hand, the existence of high stresses at the stalled oscillations with no direct resonant wake excitation manifests such a small aerodamping, which is a basic kind

of damping in the fundamental mode. As a rule the decrease of aerodamping happens near the boundary of stalled flutter. Therefore, this type of stalled oscillations may be referred as the buffeting flutter.

4. Conclusions

Blade vibration characteristics in the LP axial compressor of 100 MW heavy-duty gas turbine have been investigated at the starting conditions, using the scaled-down model compressor. It is shown that at the part loads the first lower stages of compressor operate with low flow coefficients and at the stalling incidences. The streamlining of blades with large positive incidence angles causes the occurrences of buffeting flutter, rotating stall, and surge. The characteristics of these stalled oscillations have been investigated and their exciting mechanisms have been considered. The operating modes of stages have been related to the intensities of stalled oscillations. The stalled oscillations have resulted in intensive vibrations in the fundamental flexural modes of the first and second stage blades, however, which are not resonant vibrations. They have occurred in a wide range of relative speed, $\bar{n}=0.3\sim 0.7$. Further, the resonances with stall cell excitations or with inlet strut wake excitations at the stalled conditions have caused high dynamic stress peaks in the first stage blades. The stress peaks have reached around 120 MPa.

References

- Ishihara, K. and Funakawa, M., 1980, "Experimental Investigations on the Vibration of Blades Due to a Rotating Stall," *Bulletin of the JSME*, Vol. 23, No. 177, pp. 353~360.
- Ki, J. Y. and Chung, S. C., 2002, "Performance Simulation of a Turboprop Engine for Basic Trainer," *KSME International Journal*, Vol. 16, No. 6, pp. 839~850.
- Kulagina, V. A., 1976, "Some Features of Blade Oscillations at Conditions of a Rotated Stall," *Problems of Strength, Kiev*, No. 3, pp. 45~48.
- Rusanova, E. I., 1958, "The Analysis of Mea-

surement Results of Dynamic Stresses in Blades of Axial Compressors," *Transactions of Scientifically Engineering Society of Ship Industry*, Vol. 8, No. 1, pp. 133~159.

Samoylovict, G. S., 1975, "Excitation of Blade Oscillations of Turbomachines," Moscow.

Shannon, J. F., 1954, "Vibration Problems in Gas Turbines, Centrifugal and Axial-Flow Com-

pressors," H. M. Stationary Office, London, R. and M. No. 2226.

Vedichtchev, A. F. and Titenskiy, V. I., 1983, "Heightening of Vibrational Reliability of Rotor Blades in Axial Compressors at Starting Conditions," The theses of the reports 9, All-Union Conference on Aeroelasticity Turbomachines, Novosibirsk.